The Astrophysical Journal, 575:217–224, 2002 August 10

INTERSTELLAR ABSORPTION OF THE GALACTIC POLAR LOW-FREQUENCY RADIO BACKGROUND SYNCHROTRON SPECTRUM AS AN INDICATOR OF CLUMPINESS IN THE WARM IONIZED MEDIUM

J. D. Peterson and W. R. Webber
Department of Astronomy, MSC 4500, New Mexico State University, P.O. Box 30001, Las Cruces, NM 88003; jaspeter@nmsu.edu, bwebber@nmsu.edu
Received 2001 December 6; accepted 2002 April 17

ABSTRACT

In the standard model of low-frequency synchrotron radiation propagation through the Galaxy, the absorbing warm ionized medium (WIM) is considered to be a thick slab of thermal electrons of uniform density. When the calculated polar radio spectrum is compared with the observed Galactic background radio spectrum, it is found that this model requires a much higher electron density n_e or much lower temperature T_e than permitted by current observations. A more realistic plane-parallel model, in which electron density, temperature, and cosmic-ray electron emissivity have smooth distributions with height z above the Galactic plane, is also found to suffer from the same setbacks as the standard model. However, a plane-parallel model in which the absorbing WIM has a clumpy distribution with clump densities of $\sim$0.2 cm^{-3} and filling factor of 0.08–0.15 agrees with both the low-frequency radio synchrotron spectrum and the observational parameters $\langle n_e(z=0)\rangle \approx 0.025$ cm^{-3}, $T_e \approx 7000$ K, and DM ≈ 23 pc cm^{-3}. The clumpy WIM model also supports the idea of a local interstellar cloud (LIC), which is required to provide adequate absorption below $\sim$0.5 MHz. This LIC appears to become optically thick only below $\sim$0.1 MHz where future radio measurements may be used to determine the emissivity spectrum and, therefore, the local interstellar cosmic-ray electron spectrum at energies of $\sim$40 MeV.

Subject headings: cosmic rays — ISM: clouds — ISM: structure — radiation mechanisms: nonthermal — radiative transfer

1. INTRODUCTION

The polar low-frequency background radio synchrotron spectrum of the Milky Way contains clues about the distribution of free thermal electrons in the warm ionized component of the interstellar medium (ISM) that are responsible for the absorption of electromagnetic radiation below a few MHz. Since the opacity of the warm ionized medium (WIM) depends on the path length through the disk, different frequencies exhibit the effects of absorption at different heights above the Galactic plane. Traditionally, these effects have been interpreted as variations in emissivity coupled with the absorption by a single slab of uniform thermal electron density and temperature. This paper offers a more detailed view of interstellar absorption that is consistent with Hα and pulsar dispersion measurements in which the density profile of the intervening thermal electrons is largely responsible for the shape of the observed low-frequency radio spectrum between $\sim$0.1 and 10 MHz.

As early as the 1960s, the low-frequency spectrum of the Galactic radio synchrotron background above a few MHz had been found to follow a power-law spectrum of index $\sim$0.5–0.7 between 10 and 100 MHz with a peak at about 5 MHz (Hoyle & Ellis 1963). In 1969, the satellite *Radio Astronomy Explorer 1* (*RAE 1*) observed the background radiation between 0.4 and 6.5 MHz and showed that the spectral peak in fact lies at $\sim$3 MHz (Alexander et al. 1969). Subsequent space-based observations were made, specifically by *Interplanetary Monitoring Platform 6* (*IMP 6*; Brown 1973) and *RAE 2* (Novaco & Brown 1978), which extended the known spectrum down to 100 kHz.

The data points of Figure 1 show measurements of the Galactic polar radio background between $\sim$0.1 and 500 MHz. Included in the figure are the low-frequency observations made by the *IMP 6* and *RAE 2* spacecraft below $\sim$10 MHz. The *RAE 2* data show a close agreement between the spectra of the north and south Galactic poles and a steep positive slope below $\sim$0.5 MHz. *IMP 6* also exhibits this steep spectrum that begins to flatten at frequencies just below $\sim$200 kHz, the minimum frequency detected by *RAE 2*.

This low-frequency synchrotron radio emission is produced almost entirely by cosmic-ray electrons (CREs) in the magnetic field of the Milky Way. The frequency of the radiation depends directly on the energy of the electron, and, although the emission from a single electron is spread over a broad range of frequencies, most occurs near a single critical frequency ν_c related to the CRE energy by

$$\nu_c \approx \left(\frac{E}{m_e c^2}\right)^2 \frac{qB}{2\pi m_e} \approx 54 E_{\rm GeV}^2 \ \text{MHz} \qquad (1)$$

(Longair 1994), where $E_{\rm GeV}$ is the energy of the electron in units of GeV, m_e is the mass of the electron, c is the speed of light, q is the electron charge, and B is the magnitude of the Galactic magnetic field taken to be $\sim$5 μG (Peterson et al. 1999; Rand & Kulkarni 1989). For the radio-frequency range of interest in this paper, $\sim$0.1–1000 MHz, the emitting CRE population covers the energy range of $\sim$0.05–4 GeV.

Not only is the frequency range of radio emission related to the energy range of CREs, but, given the assumption that the CREs follow a power-law distribution in energy, the radio spectral index is related to that of the CRE spectrum. Those CREs above $\sim$10 GeV are believed to represent the local interstellar spectrum (IS) since they are not significantly influenced by propagation effects within the heliosphere. The assumption of a power-law distribution of index $\sim$3.3 is consistent with CRE observations above 10

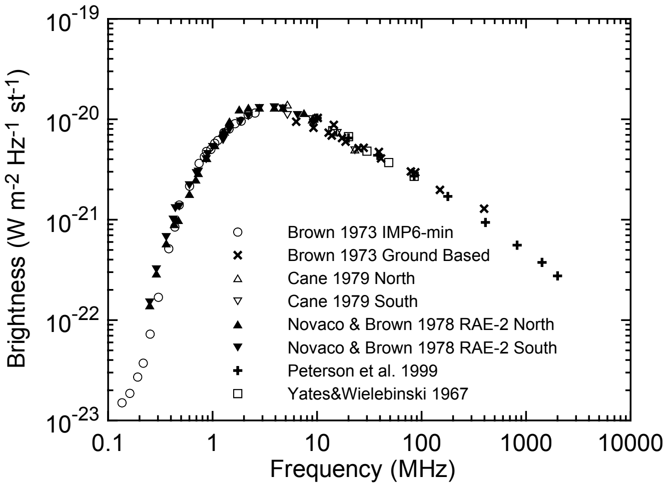

FIG. 1.—Data points represent many independent low-frequency radio observations, clearly exhibiting a peak in the spectrum at 3–4 MHz caused by free-free absorption in the WIM. The average error in the *RAE 2* spectra, not shown for clarity, amounts to roughly 20% (Novaco & Brown 1978). The average error in the *IMP 6* data is about 16% (Brown 1973). Errors in the data from both spacecraft are lower than this average value at higher frequencies and increase toward lower frequencies.

GeV, so the relationship

$$\alpha = \frac{p-1}{2} \tag{2}$$

holds for a radio spectrum of intensity $I_\nu \propto \nu^{-\alpha}$ and a CRE energy spectrum of the form $N(E)dE \propto E^{-p}$. Below 10 GeV, however, where solar modulation interferes with the passage of CREs through the heliosphere, the observed CRE energy spectrum begins to flatten (see summary by Wiebel-Sooth & Biermann 1999).

The above relation between α and p is true only for the *unabsorbed* radio spectrum, or emissivity spectrum, which is simply the volume emissivity (ε_ν) integrated along a given line of sight. The radio synchrotron spectrum above $\sim$10 MHz directly reflects this emissivity spectrum because absorption is unimportant. At lower frequencies, however, radio waves are attenuated by thermal electrons in the ISM. In this process of *free-free absorption*, radio-frequency photons are absorbed by thermal electrons in the presence of a field of positive ions. The absorption coefficient that describes the attenuation is well known:

$$\kappa_\nu = 0.0178 g_{\rm ff} \frac{n_e^2}{\nu^2 T_e^{3/2}} \ \text{cm}^{-1} , \tag{3}$$

where n_e and T_e are the density (cm^{-3}) and temperature (K) of thermal electrons, respectively, ν is measured in Hz, and $g_{\rm ff}$ is the Gaunt factor,

$$g_{\rm ff} = 10.6 + 1.9 \log T_e - 1.26 \log \nu \tag{4}$$

(Allen 1973).

Over frequencies at which free-free absorption renders the WIM completely opaque, the observed radio emission consists only of the local source function contribution $S_\nu = \varepsilon_\nu / \kappa_\nu$. At these frequencies, the emissivity spectral index differs from that of the observed radio spectrum by an additive constant of -2.1, which is the approximate frequency dependence of κ_ν.

As this paper will demonstrate, the WIM is actually completely opaque only at frequencies below 0.1 MHz. Radio emission between 0.1 and $\sim$10 MHz, above which the galaxy is transparent, probes absorption effects at various heights above the Galactic plane. Therefore, information about the height (z) distribution of the parameters n_e and T_e can be obtained from observations of the background radio spectrum in this frequency range given some a priori knowledge or assumptions about the synchrotron emissivity spectrum.

2. PARAMETERS AFFECTING LOW-FREQUENCY SYNCHROTRON EMISSION AND ABSORPTION

Independent measurements of the important Galactic parameters n_e, T_e, and ε_ν, while not exact, have been made with enough precision to establish acceptable limits. Such measurements can be used to develop a model in which the values and z-distributions of these parameters simulate Galactic conditions that produce the observed synchrotron radio background, particularly in the polar direction.

2.1. *The Thermal Electron Density*

An observation of the dispersion measure along the line of sight to a pulsar is a direct measurement of the electron column density. By making dispersion measurements toward many different pulsars of known distances, one can develop a map of average electron densities in various regions throughout the ISM. In this way, Reynolds (1991b) used a sample of high-latitude pulsars to determine a Galactic thermal electron height distribution of the form $n_e(z) = 0.015 e^{-z/70\,\text{pc}} + 0.025 e^{-z/910\,\text{pc}}$ cm^{-3}. The "thin-disk" component of this distribution represents the contribution of H II regions near the plane of the galaxy. The "thick disk" is composed of the diffuse ionized gas (DIG) that pervades the ISM. The density at the plane, $n_e(0) = 0.025 \pm 0.005$ cm^{-3}, has been deduced from low-latitude pulsars (Weisberg, Rankin, & Boriakoff 1980), while the scale height $h = 910$ (+620, -320) pc is found from the ratio of the column density (or dispersion measure) to the electron density at $z = 0$, since $\text{DM} = \int_0^\infty n_e(0) e^{-z/h}\, dz = n_e(0) h$. An average maximum dispersion measure of 6.9×10^{19} cm^{-2} was used for the scale height calculation. This value was determined from the flattening of the DM data above $\sim$1 kpc, implying that the globular cluster pulsars residing at still greater distances lie almost completely above the thermal electron population of the Galactic disk. Observations of atomic line emission in the Perseus spiral arm of the galaxy appear to confirm the electron scale height of $\sim$1 kpc deduced from the dispersion measures (Haffner, Reynolds, & Tufte 1999).

Reynolds' thermal electron z-distribution derived from DM data is not unique. Gómez, Benjamin, & Cox (2001) infer an electron profile in which $n_e(z) = 0.0071 e^{-z/50\,\text{pc}} + 0.0203 e^{-z/1070\,\text{pc}}$ cm^{-3} from a sample of 109 pulsars. The model of Taylor & Cordes (1993) employed a sample of 74 pulsars with independent distance measurements to predict $n_e(z) = 0.01875\,\text{sech}^2\,(z/880\ \text{pc})$ cm^{-3} at the radial position of the Sun in the Galaxy. So that the profile of Taylor & Cordes (1993) could be compared with the other profiles examined in this paper, it was fitted with an exponential function from $z = 0$ to 1.5 kpc yielding $n_e(z) = 0.026 e^{-z/685\,\text{pc}}$ cm^{-3}. Based solely on a least-squares fit to yet another sample of pulsar dispersion measure data, Nordgren, Cordes, & Terzian (1992) found $n_e(z) = 0.033e^{-z/670\,\mathrm{pc}}$ cm^{-3}. Giving equal weight to all four of the above thermal electron profiles, this paper employs an average electron z-distribution of

$$n_e(z) \approx 0.025e^{-z/830\,\mathrm{pc}}\ \mathrm{cm}^{-3}\ , \tag{5}$$

ignoring the thin-disk components of Reynolds (1991b) and Gómez et al. (2001).

Obviously, thermal electron profiles based on dispersion measures are ambiguous; a uniform, exponential, Gaussian, or any other arbitrary distribution can produce the same value of the DM with the appropriate choice of path length. Fortunately, the emission measure (EM) along the line of sight can add constraints to the distribution. It is defined by

$$\mathrm{EM} = \int n_e^2\, ds \approx 2.75 T_4^{0.9} I_\alpha\ \mathrm{cm}^{-6}\ \mathrm{pc}\ , \tag{6}$$

where T_4 is the temperature in units of 10^4 K and is usually taken to be 0.8 (Reynolds 1989) and I_α is the Hα intensity in rayleighs (1 R $= 10^6/4\pi$ photons cm^{-2} s^{-1} sr^{-1}; Reynolds 1991a). Because it depends on the *square* of the electron density, it is particularly sensitive to concentrated ionized regions.

Both emission and dispersion measurements have been made toward four high-latitude pulsars that reside more than 3 kpc away from the Galactic plane (Reynolds 1991a), which give averages $\langle \mathrm{EM}|\sin b| \rangle = 2.0 \pm 0.3$ pc cm^{-6} and $\langle \mathrm{DM}|\sin b| \rangle = 22.7 \pm 2.6$ pc cm^{-3} [$(7.0 \pm 0.8) \times 10^{19}$ cm^{-2}; Reynolds 1997]. If a uniform thermal electron distribution is assumed, the average density at the Galactic plane calculated from these values is 0.088 cm^{-3} and the disk thickness is 260 pc, much too high and too low, respectively, relative to the values proposed in any of the aforementioned electron profiles. The electron density at the plane $n_e(0)$ and the scale height h deviate even further from the above assumed values if an exponential electron distribution is assumed, yielding 0.18 cm^{-3} and 130 pc, respectively. Since dense regions contribute more to the EM than to the DM, the solution to this discrepancy may be that the WIM is "clumpy" with relatively dense ($\sim$0.1–0.3 cm^{-3}) clouds occupying $\sim$200–300 pc throughout a disk half-thickness of $\sim$1 kpc, resulting in a filling factor $\sim$0.1–0.3 (Reynolds 1991a; Kulkarni & Heiles 1987). In this case, the profile of equation (5) would represent the space-averaged profile $\langle n_e(z) \rangle$.

Another possible solution is that a thinner, denser component of the thermal electron distribution exists in addition to the thick disk. The thin-disk component of Reynolds (1991b), although it still does not satisfy both EM and DM averages above, adds only 5% to DM while it boosts EM by 28% over the contribution of the thick disk alone. In order to maintain the thick disk of equation (5) yet still agree with the observed DM and EM, the second component would require the electron density at the Galactic plane to be 2.6 cm^{-3} with a scale height of 0.5 pc. The fact that this high density at $z = 0$ disagrees with the measurements of Weisberg et al. (1980) by 2 orders of magnitude lends credence to the "clumpy WIM" model mentioned above, and because of this, a dense thin-disk component will not be considered further in this paper.

2.2. *The Thermal Electron Temperature*

The temperature of the WIM is commonly accepted to be $\sim$8000 K, deduced from observations of the widths of collisionally excited atomic emission lines (Reynolds 1985). The allowable temperature range is fairly broad, however, as the ratio of emission measure to free-free opacity at 10 MHz suggests that T_e may be as low as 4400 K (Kulkarni & Heiles 1987). Observations of [N II] and Hα emission line ratios in the Perseus Arm of the Milky Way suggest that there is a height variation by which the electron temperature increases from $\sim$7000 K at $z \approx 500$ pc to $\sim$11,000 K at $z \approx 1500$ pc (Reynolds, Haffner, & Tufte 1999). The resulting temperature distribution can be well approximated by the quadratic polynomial $T_e = 7000 - 0.526z + 0.00177z^2$ K, where z is in parsecs. However, because this function for $T_e(z)$ only increases to $\sim$8000 K at 1 scale height of the thermal electron disk ($\sim$1 kpc), a uniform T_e profile of 7000 K will be adopted for the calculations in this study.

2.3. *The Synchrotron Volume Emissivity*

The volume emissivity of synchrotron radiation due to Galactic CREs has been measured by observing radio frequencies along lines of sight toward H II regions (e.g., Kassim 1990; Caswell 1976; Rockstroh & Webber 1978). These highly ionized zones are opaque to any low-frequency radiation originating from behind them; therefore, observed radio emission toward an H II region is entirely due to the emissivity of CREs between it and Earth. The ratio of the observed intensity to the distance to an H II region gives the mean volume emissivity along the line of sight. A simple average calculated from Caswell's measurements at 10 MHz yields an emissivity $\langle \varepsilon_{10\,\mathrm{MHz}} \rangle = (2.4 \pm 0.7) \times 10^{-40}$ W m^{-3} Hz^{-1} sr^{-1} for H II regions that lie between $\sim$450 pc and $\sim$2.2 kpc from Earth. Because these regions are somewhat distant, this mean emissivity probably does not accurately reflect that of the local CRE population. To compensate for this, Fleishman & Tokarev (1995) noted a roughly linear relationship between the emissivity and the line-of-sight distances in which the average emissivity tends to be lower for more distant H II regions. Using the data of Caswell (1976), Andrew (1969), and Ellis (1982), they extrapolated this relationship to obtain a local $z = 0$ value of $\varepsilon_{10\,\mathrm{MHz}} = 3.0 \times 10^{-40}$ W m^{-3} Hz^{-1} sr^{-1}.

The synchrotron emissivity decreases with respect to its value at the Galactic plane as z is increased since the parameters that dictate it, namely, the CRE flux and the magnitude of the Galactic magnetic field, also diminish with height above the plane (Kulkarni & Heiles 1988). In external galaxies, where we can view the entire system as a whole, this trend is easily observable. Some galaxies exhibit a double-exponential profile, consisting of both a thin- and thick-disk component (e.g., NGC 891, Allen, Baldwin, & Sancisi 1978; Hu et al. 1987; NGC 4565, Naeslund & Joersaeter 1997; NGC 4631, Dahlem, Lisenfeld, & Golla 1995). To search for clues to the emissivity distribution in our own Galaxy, a 408 MHz all-sky survey was analyzed by Beuermann, Kanbach, & Berkhuijsen (1985) since the unabsorbed synchrotron emissivity spectrum dominates at this frequency. Close agreement between the data and a two-component model of the vertical emissivity profile suggests that the Milky Way, too, has both a thin and thick disk of emission. Beuermann et al. (1985) deduced scale heights for these two components of 185 ± 25 and 1800 ± 200 pc, respectively, at the radial position of the solar system in the Galaxy. The contribution of the thin disk to the total power is estimated at about 10%, which implies that the thin and thick components are responsible for 52% and 48%, respectively, of the emissivity at the plane.

Not only is the emissivity expected to vary with z, but if the local interstellar CRE spectrum begins to flatten at low energies, as expected from increased energy losses due to ionization, then the emissivity spectral index should also decrease at low frequencies. Using a Monte Carlo diffusion model of CRE propagation through the Milky Way, Higbie et al. (1999) found an average of $\sim$1.6 for the calculated interstellar CRE spectral index between 10 and 100 MeV. This implies that for the corresponding frequencies between $\sim$5 and 500 kHz, the spectral index of the synchrotron emission may flatten to a value of $\sim$0.3 via equation (2). Representing this varying spectral index by $\alpha(\nu)$, the final emissivity profile can be approximated by $\varepsilon_\nu(z) \approx \varepsilon_0^{-\alpha(\nu)}(0.52e^{-z/185\,\mathrm{pc}} + 0.48e^{-z/1800\,\mathrm{pc}})$.

3. THE STANDARD MODEL OF SYNCHROTRON RADIATION TRANSPORT

The standard model that has been used to deduce information about the emissivity spectrum (and thus the CRE spectrum; Peterson et al. 1999), given the observed radio spectrum, relies on some simple assumptions about the structure of the ISM. Among those assumptions are the following: (1) n_e, T_e, and ε_ν are constant throughout the disk of the galaxy; (2) ε_ν and κ_ν are coincident; i.e., the matter disk is uniformly mixed with CRE disk; and (3) α_ν is constant over all frequencies (e.g., Hoyle & Ellis 1963; Webber 1968; Alexander et al. 1970; Fleishman & Tokarev 1995).

The above assumptions provide a simple solution to the equations of radiative transfer because both ε_ν and κ_ν (and therefore S_ν) are constant throughout the Galactic disk. The intensity I_ν at the Galactic plane can then be written as

$$I_\nu = \frac{\varepsilon_\nu}{\kappa_\nu}(1 - e^{-\tau_\nu}) + I_{\mathrm{eg},\nu}e^{-\tau_\nu} , \qquad (7)$$

where $I_{\mathrm{eg},\nu}$ is the extragalactic component of emission, estimated to peak at a value 20% of I_ν at $\sim$3.5 MHz. The slope of this extragalactic component is also much steeper than the Galactic component ($\alpha_{\mathrm{eg}} = 0.8$; Simon 1977; Cane 1979; Dulk et al. 2001), so its contribution at much higher frequencies is insignificant. The same is true at frequencies below a few MHz where free-free absorption in the Milky Way and synchrotron self-absorption almost completely eliminate the extragalactic component before it reaches the Galactic plane.

The contribution of extragalactic sources to the radio background spectrum is given by the dotted curve of Figure 2, as proposed by Simon (1977) and later by Dulk et al. (2001). This extragalactic component is incorporated into the short-dashed curve that shows the polar radio spectrum predicted by the standard model with the values of the parameters examined in the previous section, $n_e = 0.025$ cm^{-3}, $T_e = 7000$ K, and $\varepsilon_{10} = 3 \times 10^{-40}$ W m^{-3} Hz^{-1} sr^{-1}. It is obvious that the standard model lacks enough opacity at low frequencies to fit the observed radio spectral peak unless the absorption coefficient is increased beyond that which arises from these observational parameters. The spectrum given by the solid curve shows how κ_ν can be increased such that the frequency of the turnover coincides with that of the radio synchrotron observations, in this example, by adjusting the values of the parameters to $n_e = 0.08$ cm^{-3}

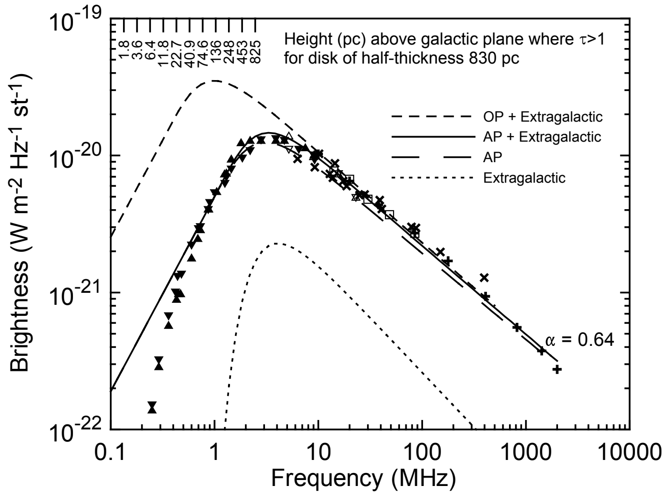

FIG. 2.—Short-dashed curve illustrates the standard model predictions of the Galactic polar synchrotron spectrum arising from the observed parameters (OP) discussed in § 2 of the paper and includes the extragalactic component (*dotted curve*) given by Dulk et al. (2001). The solid curve shows the spectrum derived from adjusted parameters (AP) such that the calculated peak frequency matches that of the observed radio data. The effective absorption path length (in parsecs) given in the top scale shows that the WIM is locally opaque only below $\sim$0.1 MHz.

and $T_e = 6000$ K. In either case, the WIM is transparent above $\sim$10 MHz so that the emissivity spectrum $I_\nu = \int_0^L \varepsilon_\nu\, dl$ dominates (where L is the half-thickness of the Galactic disk), thus constraining the spectral index of the Galactic component of I_ν to be $\alpha = 0.64 \pm 0.05$, the same as that for ε_ν, which corresponds to a CRE spectral index of $\sim$2.3 above $\sim$500 MeV. Between $\sim$0.1 and a few MHz, the absorption path length for which $\tau_\nu = 1$ ranges from a few parsecs to the thickness of the Galactic disk, as shown by the top scale in Figure 2. Therefore, the distribution of $\kappa_\nu(z)$ should affect I_ν in this frequency range, but its influence is not seen in the standard model since it is assumed that S_ν does not vary with z. For the standard model, the local source function $S_\nu(z \approx 0)$ dominates at frequencies lower than 1 MHz, and since $\kappa_\nu \propto \nu^{-2.1}$, the spectral index in this region is $\alpha - 2.1$.

The standard model also has implications for the values of n_e, T_e, $\varepsilon_{10\,\mathrm{MHz}}$, and L necessary to fit the turnover frequency. At 10 MHz, the Galactic disk is almost completely transparent so that the synchrotron intensity in the polar direction due to Galactic CREs is $I_{10,\mathrm{gal}} = \varepsilon_{10}L$. For the measured value of $I_{10,\mathrm{gal}} = 8 \times 10^{-21}$ W m^{-2} Hz^{-1} sr^{-1}, an emissivity of $\varepsilon_{10} = (2\text{–}4) \times 10^{-40}$ W m^{-3} Hz^{-1} sr^{-1} independent of z leads to disk thicknesses between 1325 and 650 pc, respectively. Using this relationship between $I_{10,\mathrm{gal}}$, ε_{10}, and L, the opacity $\tau_\nu \propto Ln_e^2T_e^{-1.5}$ can be written as $\tau_\nu \propto \varepsilon_{10}^{-1}n_e^2T_e^{-1.5}$. Because the value of the opacity τ_{peak} is directly related to the frequency of the spectral peak, it can be fixed by requiring that the model turnover coincides with that of the observed spectrum. Therefore, the ratio $n_e^2T_e^{-1.5}$ can be treated as a function of ε_{10} for models that fit the turnover frequency. Figure 3 shows the standard model value of $n_e^2T_e^{-1.5}$ required to fit the frequency of the observed radio peak for the emissivity range given above. The results of this analysis demonstrate that the standard model cannot simultaneously reproduce the peak in the radio spectrum

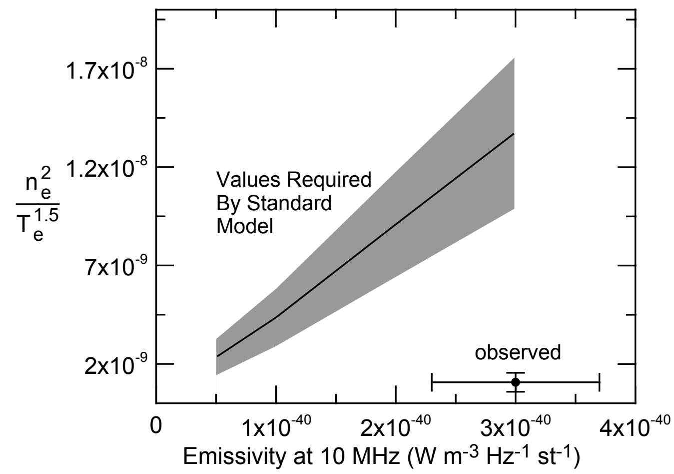

FIG. 3.—Optimum values for the ratio $n_e^2 T_e^{-1.5}$ as a function of emissivity at 10 MHz that are required to fit the predicted standard model spectral peak to that of the observed spectrum given by the solid line. Acceptable values fall within the shaded region for errors in n_e and T_e of ± 0.005 cm^{-3} and ± 1000 K, respectively. The observed value is calculated from $n_e = 0.025$ cm^{-3} and $T_e = 7000$ K.

and the observed values of n_e, T_e, and $\varepsilon_{10\,\mathrm{MHz}}$. This inconsistency can only be reconciled by accepting one or more of the following changes in the average values currently allowed by existing observations: $\langle n_e \rangle$ is much higher than 0.025 cm^{-3} (Reynolds 1989), $\langle T_e \rangle$ is much lower than 7000 K (Reynolds et al. 1999), or $\langle \varepsilon_{10} \rangle$ is much lower than $\sim 3 \times 10^{-40}$ W m^{-3} Hz^{-1} sr^{-1} (Fleishmann & Tokarev 1995).

4. A NEW MODEL FOR THE TRANSPORT OF SYNCHROTRON RADIATION

4.1. *The Basis of the New Model*

The standard model is not well suited to simulate radio synchrotron transport through the ISM for several reasons. As discussed previously, the thermal electron density and temperature may vary with height above the Galactic plane. The emissivity also appears to vary with height, and its spectral index may change with frequency. Most importantly, because the disk becomes fully opaque only at frequencies below ~ 0.1 MHz, the shape of the observed intensity spectrum between this frequency and about 3 MHz is likely to be affected by the distribution of n_e, T_e, and ε_ν. The standard model only accounts for rough averages of these values and, as such, cannot accurately reproduce a realistic low-frequency radio spectrum while agreeing with observed values of ε_ν, T_e, n_e, DM, and EM.

Our model of radio synchrotron transport is structured similarly to a simple, plane-parallel atmospheric propagation code. The Galaxy is divided into thin layers, the Galactic plane being the lowermost boundary of the disk. Within each layer, n_e, T_e, and ε_ν are constant, and therefore τ_ν is also constant. The solution to the radiative transfer equations again simplifies to a form similar to equation (7) except, for each layer but the outermost, $I_{\mathrm{eg},\nu}$ is replaced by the radiation received from the layer immediately above it. For a model of n layers, 1 being the nearest to the plane of the galaxy and n being the farthest out into the halo,

$$\begin{aligned} I_n &= \frac{\varepsilon_n}{\kappa_n}(1 - e^{-\tau_n}) + I_{\mathrm{eg}} e^{-\tau_n} \;, \\ I_{n-1} &= \frac{\varepsilon_{n-1}}{\kappa_{n-1}}(1 - e^{-\tau_{n-1}}) + I_n e^{-\tau_{n-1}} \;, \\ &\vdots \\ I_1 &= \frac{\varepsilon_1}{\kappa_1}(1 - e^{-\tau_1}) + I_2 e^{-\tau_1} \;, \end{aligned} \tag{8}$$

where I_j is the intensity of radiation received at the bottom of the jth layer and ε_j, κ_j, and τ_j are the values of the emissivity, absorption, and opacity, respectively, within the jth layer. These equations are repeated for each frequency of interest, yielding the synchrotron spectrum observed at Earth, $I_1(\nu)$. At the cost of computing time, the layer thickness can be arbitrarily reduced to the extent that any z-distribution of the aforementioned parameters can be approximated. The results of this paper were calculated using 8000 layers, corresponding to changes in the emissivity and thermal electron density on the scale of 1 pc.

4.2. *A Smoothly Distributed WIM*

The emissivity profile discussed previously, $\varepsilon(z) \approx \varepsilon_0^{-\alpha(\nu)}(0.52e^{-z/185\,\mathrm{pc}} + 0.48e^{-z/1800\,\mathrm{pc}})$, uses the spectral indices below 10 MHz derived from the Galactic CRE spectrum calculated by Higbie et al. (1999), and α_ν is set to the constant value 0.64 above 10 MHz to correspond to the direct radio measurements at those frequencies.

The remaining parameters of the model are $n_e(z)$ and T_e. A constant temperature of 7000 K is chosen for reasons mentioned previously in this paper, leaving the thermal electron density z-distribution the only free parameter in the model. The curve of Figure 4a shows the effect of selecting the average smooth exponential thermal electron profile

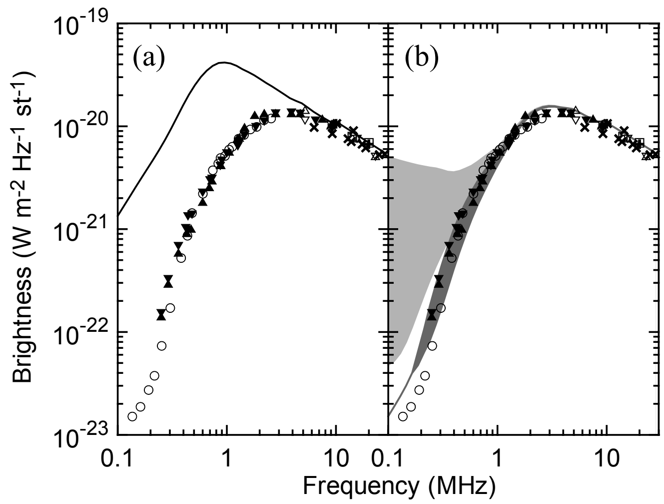

FIG. 4.—(a) Solid curve is the model spectrum resulting from the smoothly distributed electron profile of eq. (5), $n_e(z) = 0.025e^{-z/830\,\mathrm{pc}}$ and $T_e = 7000$ K. (b) Light shaded region shows the possible values for the calculated spectrum assuming a clumpy medium and has a width of 2 σ parallel to the brightness axis corresponding to the deviation of the spectra that arises from the random sampling of clumps from eq. (5). The dark shaded region shows the spectra derived from the same set of parameters as the light region except that a local cloud of 2 pc has been added.

$n_e(z) = 0.025e^{-z/830\,\mathrm{pc}}$. The peak of the calculated spectrum occurs at $\sim$1 MHz, a frequency much too low to provide an adequate fit to the observed radio synchrotron intensity. A closer fit to the data can be obtained by increasing the amount of Galactic free-free absorption, which may be accomplished by either raising the thermal electron density, lowering the temperature, or some combination of the two. For example, the peak could be fitted by both increasing the density by a factor of $\sim$3 and reducing the temperature from 7000 to 5000 K. Although the frequency of the turnover would then coincide with the observations, the thermal electron temperature and density at the Galactic plane would not. This example illustrates that the same problem that plagues the standard single-slab model is also present in the smooth, multilayer exponential thermal electron distributions. It is clear that the smooth thermal electron z-distributions still cannot account for the values of n_e and T_e while simultaneously fitting the peak in the radio spectrum. Furthermore, the shape of the model spectrum below the peak is simply not a satisfactory fit to the observed spectrum.

4.3. *A Clumpy WIM*

Obviously, what is needed is a means of increasing absorption so that the spectral peak can be fitted without raising the average electron density beyond that deduced by pulsar dispersion measurements. To accomplish this, we represent the WIM as dense layers with a filling factor $\phi(z)$ such that

$$\langle n_e(z) \rangle = n_{\mathrm{clump}}(z)\phi(z) \tag{9}$$

(Kulkarni & Heiles 1987). For simplicity, we shall assume that all clumps have the same density so equation (9) can be rewritten as

$$\left\langle n_e(0)e^{-z/h} \right\rangle = n_{\mathrm{clump}}\phi(0)e^{-z/h} \ , \tag{10}$$

where h is the scale height chosen for the thermal electron profile. The requirement that the model fit the observed spectral peak frequency effectively fixes n_{clump} so the only remaining free parameter of equation (10) is the choice of the average thermal electron profile.

The model simulates a clumpy medium by assigning to each layer a density of either n_{clump} or zero. Whether or not a specific layer represents a clump is decided by randomly sampling the adopted thermal electron profile. The probability that a given layer is assigned the properties of a clump is given by the filling factor $\phi(z)$, which decreases exponentially with z such that equation (10) is satisfied. The model was run 100 times to obtain a spectrum with a statistically significant mean and deviation in order to account for the effects of the random clump placement. Because individual layers are chosen to represent clumps, their size and quantity depend on the total number of layers in the model. The physical thickness of the exponential disk was taken to be 8 kpc, a factor of 5 greater than the scale height of the thick emissivity disk, which is the most extended component of the model. With this choice, the emissivity and electron density both become nearly zero at the outer boundary of the disk. The calculated spectrum only begins to approach the observed data when more than $\sim$1000 layers are input into the model; hence, because the total extent of the disk is taken to be 8 kpc, this suggests an upper limit to the clump size of $\sim$8 pc. The mean derived from individual model spectra arising from different random clump placements does not change significantly if the number of layers is increased beyond 1000. Furthermore, the deviation of the individual spectra from the mean decreases as the number of layers increases.

The light shaded region of Figure 4*b* shows the spectrum within 1 σ above and below the mean that arises from a clump density of 0.225 cm^{-3}, a filling factor of 0.11, and the average electron profile of equation (5). There is little variation in the spectrum above a few MHz because emission at such frequencies is not significantly absorbed by the interstellar thermal electrons, so the placement of clumps does not affect the spectrum at higher frequencies. Using the clumpy WIM model, the turnover frequency in the model spectrum now fits the peak in the observed radio data, and at the same time the required model parameters $\langle n_e(0) \rangle = 0.025 \pm 0.005$ cm^{-3}, $T_e \approx 7000$ K, DM ≈ 23 pc cm^{-3}, and $\varepsilon_{10}(0) = 3 \times 10^{-40}$ W m^{-3} Hz^{-1} sr^{-1} almost exactly correspond to the observed values.

The emission measure of 4.5 ± 0.6 pc cm^{-6} derived from this clumpy model, however, is about a factor of 2 greater than the observations. Because the emission measure and the opacity both depend on n_e^2, both τ_ν and EM are constrained by the requirement that the peaks of the model spectrum and observed spectrum coincide. In this way, the turnover in the low-frequency radio spectrum is, essentially, an independent means of determining EM. Although this value is a factor of $\sim$2 larger than that derived from Hα observations, it remains a significant improvement over the smooth exponential thermal electron models that predict the emission measure to be too low by a factor of $\sim$10.

Despite the good agreement between the model and observed spectral peaks, there is evidently still not enough absorption at the lowest frequencies. In fact, the mean model spectrum begins to rise with decreasing frequency below 0.2 MHz. This is because the probability of having a clump at $z = 0$ is given by $\phi(0) \sim 0.1$; therefore, the random sampling produced an average of one clump within about 10 pc of the Galactic plane. Since the model assumes that there are no thermal electrons outside the clumps, there is no local absorption at these frequencies. Thus, the emissivity begins to dominate such that the intensity increases with decreasing frequency because of the negative slope of the CRE spectrum.

The solution to this disagreement is simply to place a clump with an extent of a few parsecs at our location in the Galaxy. Considerable evidence exists to support this kind of solution. Korsakov, Tokarev, & Fleishman (1997) have proposed a local absorption feature of thermal electron density 0.3 cm^{-3} to explain the features of the low-frequency radio spectrum. The agreement between absorption-line measurements and models of the local interstellar ionizing radiation field indicates that the electron density of the local interstellar cloud (LIC) in which the solar system is embedded is on the order of 0.1 cm^{-3} (Frisch 1998). Gry & Jenkins (2001) used absorption features in the UV spectrum of the star gCMa to derive parameters for the LIC: $n_e = 0.12 \pm 0.05$ cm^{-3}, $T_e = 7000 + 1200$ K, and the line-of-sight distance through the cloud toward gCMa is on the order of 1 pc. Although the model was tested with a local clump of density 0.12 cm^{-3}, it resulted in too little absorption below $\sim$1 MHz. However, the addition of a slightly more dense clump significantly influences radio absorption at the lowest frequencies while leaving unchanged the values of the parameters $\langle n_e \rangle$, T_e, DM, EM, and $\varepsilon_{10}(0)$ specified at the beginning of this section. The dark shaded region of Figure 4*b* has the same parameters as the light region with the exception that a local interstellar cloud 2 pc in size has been added with density of 0.225 cm^{-3}. The clumpy model spectrum is now in very good agreement with the observed polar radio spectrum measured by *RAE 2*, including the steep spectral falloff of index greater than $\alpha - 2.1$ below $\sim$0.5 MHz that cannot be reproduced in models with uniform or smooth exponential z-distributions of thermal electrons.

An interesting prediction of this clumpy WIM model is the flattening of the spectrum below $\sim$0.2 MHz. Although the *IMP 6* data points that portray this flattening in the observed spectrum may be questionable because of measurement errors, such behavior is expected at frequencies below $\sim$0.2 MHz because of the short optical path length (<1 pc) due to absorption by the local clump. Because of this high opacity, the observed spectrum at these frequencies is simply given by the local source function S_ν, which is a power law of index $\alpha - 2.1$. Accurate measurements in this frequency range, therefore, might be used to determine the spectral index α of the local CRE energy distribution below $\sim$40 MeV.

5. SUMMARY AND CONCLUSIONS

Because the Galactic polar low-frequency background radio spectrum below a few MHz is primarily shaped by free-free absorption in the ISM, it is significantly affected by the z-distribution of thermal electrons in the WIM of the Milky Way. In this study, we have recovered information about the WIM through the use of a synchrotron radiation propagation model in which different WIM distributions can be represented. A successful model must reproduce features of the observed radio spectrum while remaining consistent with observed thermal electron properties: $\langle n_e(0) \rangle \approx 0.025$ cm^{-3} with a disk thickness or scale height of $\sim$1 kpc, $T_e \approx 7000$ K, DM ≈ 23 pc cm^{-3}, and EM ≈ 2 pc cm^{-6}.

The standard model typically utilized to simulate the propagation of synchrotron radiation through the Galaxy has been selected because of its simplicity; it assumes that the Milky Way is a thick slab of thermal electrons of uniform temperature and density. To fit the frequency of the peak of the observed radio spectrum using this model, however, one must choose values of n_e (and thus DM and EM) and T_e that significantly disagree with the independently measured values stated above. This implies that modifications to the standard model are needed.

The model presented in this paper allows for variations in $n_e(z)$ and $\varepsilon_\nu(z)$ by dividing the thick slab that represents the Milky Way in the standard model into 8000 plane-parallel layers. We find that a smooth, exponentially decreasing thermal electron density z-distribution is still incapable of simultaneously reproducing the peak in the observed radio spectrum and maintaining $n_e(0)$ and T_e within ranges allowed by observation. If, instead, a clumpy WIM distribution is inserted into the model, then the *average* value of the electron density can be maintained while increasing n_e^2, thereby allowing more freedom in fitting the spectral peak frequency.

For a clumpy distribution with a clump density of 0.225 cm^{-3}, a filling factor of 0.11, and the average electron profile of equation (5), the frequency of the spectral peak can be fitted while simultaneously maintaining the measured values of the parameters n_e, T_e, ε_{10}, and DM stated at the beginning of this section. The emission measure resulting from this model also agrees more closely with the observations, being only a factor of $\sim$2 too high rather than a factor of $\sim$10 too low as predicted by the smooth WIM distributions. The calculated radio spectrum below $\sim$1 MHz, however, still diverges significantly from the observed data unless the model includes a local clump of density 0.225 cm^{-3} that surrounds the solar system with a radial extent of about 2 pc. This results in a good model spectrum fit to the low-frequency radio data, even below $\sim$0.5 MHz.

The clumpy WIM model also predicts the flattening of the spectrum seen in the *IMP 6* data below $\sim$0.2 MHz as a result of the local clump becoming optically thick to low-frequency radiation. At lower frequencies, it is likely that the local source function S_ν dominates so that the spectral index approaches $\alpha - 2.1$. Thus, future measurements of the radio spectrum below $\sim$0.2 MHz are possibly the only way to obtain information about the emissivity spectrum in this frequency range and, consequently, the low-energy cosmic-ray electron energy distribution.

The authors would like to thank René Walterbos for his discussion and comments during the preparation of this work.

REFERENCES

Alexander, J. K., Brown, L. W., Clark, T. A., & Stone, R. G. 1970, A&A, 6, 476
Alexander, J. K., Brown, L. W., Clark, T. A., Stone, R. G., & Weber, R. R. 1969, ApJ, 157, L163
Allen, C. W. 1973, Astrophysical Quantities (3d ed.; London: Athlone)
Allen, R. J., Baldwin, J. E., & Sancisi, R. 1978, A&A, 62, 397
Andrew, B. H. 1969, MNRAS, 143, 17
Beuermann, K., Kanbach, G., & Berkhuijsen, E. M. 1985, A&A, 153, 17
Brown, L. W. 1973, ApJ, 180, 359
Cane, H. V. 1979, MNRAS, 189, 465
Caswell, J. L. 1976, MNRAS, 177, 601
Dahlem, M., Lisenfeld, U., & Golla, G. 1995, ApJ, 444, 119
Dulk, G. A., Erickson, W. C., Manning, R., & Bougeret, J.-L. 2001, A&A, 365, 294
Ellis, G. R. A. 1982, Australian J. Phys., 35, 91
Fleishman, G. D., & Tokarev, Y. V. 1995, A&A, 293, 565
Frisch, P. C. 1998, Space Sci. Rev., 86, 107
Gómez, G. C., Benjamin, R. A., & Cox, D. P. 2001, AJ, 122, 908
Gry C., & Jenkins, E. B. 2001, A&A, 367, 617
Haffner, L. M., Reynolds, R. J., & Tufte, S. L. 1999, ApJ, 523, 223
Higbie, P. R., Peterson, J. D., Rockstroh, J. M., & Webber, W. R. 1999, Proc. 26th Int. Cosmic-Ray Conf. (La Jolla), 4, 245
Hoyle, F., & Ellis, R. A. 1963, Australian J. Phys., 16, 1
Hu, F. X., Allen, R. J., van der Kruit, P. C., & You, J. H. 1987, Ap&SS, 135, 389
Kassim, N. E. 1990, in Low Frequency Astrophysics from Space, ed. N. E. Kassim & K. W. Weiler (Berlin: Springer), 144
Korsakov, B. G., Tokarev, Yu. V., & Fleishman, G. D. 1997, Astron. Lett., 23, 229
Kulkarni, S. R., & Heiles, C. 1987, in Interstellar Processes, ed. D. J. Hollenbach & H. A. Thronson, Jr. (Dordrecht: Reidel), 87
———. 1988, in Galactic and Extragalactic Radio Astronomy, ed. G. L. Verschuur & K. I. Kellermann (New York: Springer), 95
Longair, M. S. 1994, High Energy Astrophysics, Vol. 2 (2d ed.; Cambridge: Cambridge Univ. Press)
Naeslund, M., & Joersaeter, S. 1997, A&A, 325, 915
Nordgren, T. E., Cordes, J. M., & Terzian, Y. 1992, AJ, 104, 1465
Novaco, J. C., & Brown, L. W. 1978, ApJ, 221, 114
Peterson, J. D., Higbie, P. R., Rockstroh, J. M., & Webber, W. R. 1999, Proc. 26th Int. Cosmic-Ray Conf. (La Jolla), 4, 251
Rand, R. J., & Kulkarni, S. R. 1989, ApJ, 343, 760
Reynolds, R. J. 1985, ApJ, 294, 256
———. 1989, ApJ, 345, 811
———. 1991a, ApJ, 372, L17
———. 1991b, in IAU Symp. 144, The Interstellar Disk-Halo Connection in Galaxies, ed. H. Bloemen (Dordrecht: Kluwer), 67

Reynolds, R. J. 1997, in The Physics of Galactic Halos, ed. H. Lesch, R.-J. Dettmar, U. Mebold, & R. Schlickeiser (Berlin: Akademie), 57
Reynolds, R. J., Haffner, L. M., & Tufte, S. L. 1999, ApJ, 525, L21
Rockstroh, J. M., & Webber, W. R. 1978, ApJ, 224, 677
Simon, A. J. B. 1977, MNRAS, 180, 429
Taylor, J. H., & Cordes, J. M. 1993, ApJ, 411, 674
Webber, W. R. 1968, Australian J. Phys., 21, 845
Weisberg, J. M., Rankin, J. M., & Boriakoff, V. 1980, A&A, 88, 84
Wiebel-Sooth, B., & Biermann, P. L. 1999, in Landolt-Börnstein—Astronomy and Astrophysics, VI/3C (Berlin: Springer), 83
Yates, K. W., & Wielebinski, R. 1967, ApJ, 149, 439